

# Experimental and Theoretical Studies on the Magnetic Circular Dichroism of Azanaphthalenes. Use of the CNDO/S-CI Approximation

Akira Kaito and Masahiro Hatano\*

Contribution from the Chemical Research Institute of Non-aqueous Solutions, Tohoku University, Sendai 980, Japan. Received November 1, 1977

**Abstract:** The magnetic circular dichroism (MCD) spectra of quinoline, isoquinoline, quinoxaline, phthalazine, quinazoline, cinnoline, and pyrido[2,3-*b*]pyrazine were measured in the wavenumber region of 20 000–50 000 cm<sup>-1</sup>. The transition energies, the oscillator strengths, and the Faraday *B* terms calculated within the framework of the CNDO/S-CI approximation are in reasonable agreement with the experimental results, which permits us to discuss the spectral assignment. The signs of the Faraday *B* terms of two lowest  $\pi^* \leftarrow \pi$  transitions are found to be changed according to whether the aza substitution occurs at the  $\alpha$  or  $\beta$  position. The origins for the Faraday *B* terms of the lowest allowed  $\pi^* \leftarrow n$  transition and two lowest  $\pi^* \leftarrow \pi$  transitions were also investigated.

In recent years, considerable attention has been paid to the electronic structure of azanaphthalenes.<sup>1-4</sup> The electronic spectra of azanaphthalenes were interpreted on the basis of the semiempirical SCF-MO calculations.<sup>1-3</sup> The photoelectron spectra of azanaphthalenes were measured, and the ordering of the occupied  $\pi$  orbitals and the nitrogen lone pair orbitals was discussed.<sup>4</sup> In spite of these theoretical and experimental works, there are some unsettled problems regarding the spectral assignments.

The replacement of a CH group by a nitrogen atom not only causes the  $\pi^* \leftarrow n$  transitions in the lower wavenumber region, but also modifies the  $\pi^* \leftarrow \pi$  states of the naphthalene. The absorption spectra of the azanaphthalenes are changeable according to whether the aza replacement occurs at the  $\alpha$  or  $\beta$  position.<sup>2</sup> The highest occupied  $\pi$  molecular orbital (HOMO) and the lowest unoccupied  $\pi$  molecular orbital (LUMO) of naphthalene are more sensitive to the  $\alpha$ -aza substitution than the  $\beta$ -aza substitution.<sup>3</sup>

On the other hand, the magnetic circular dichroism (MCD) technique has been extensively studied as a useful tool for the investigation of the electronic structures of organic aromatic molecules. The electronic structures of naphthalene has been compared with those of its isomeric hydrocarbon, azulene, from the MCD point of view.<sup>5</sup> Recently, Michl<sup>6</sup> has explained the signs of the Faraday *B* terms of the lowest  $\pi^* \leftarrow \pi$  transition of the heteroatom analogues of naphthalene and other alternant hydrocarbons, on the basis of the Pariser-Parr-Pople model.<sup>7</sup> Although Michl's treatment has succeeded in explaining the signs of the MCD of various aromatic compounds, he has considered only  $\pi$  electrons.

On the other hand, the complete neglect of differential overlap (CNDO),<sup>8,9</sup> all valence-electron LCAOMO-SCF procedure is superior to the  $\pi$ -electron approximation in that the CNDO method is applicable to evaluating the magnetic mixing between  $\pi^* \leftarrow \sigma$  and  $\pi^* \leftarrow \pi$  states and to dealing with the Faraday *B* terms of the  $\pi^* \leftarrow n$  transitions. The Faraday *B* terms of some alternant hydrocarbons,<sup>10</sup> adenines,<sup>11</sup> formaldehyde,<sup>12</sup> benzene itself,<sup>13,14</sup> indole,<sup>15</sup> azabenzene,<sup>16</sup> and monosubstituted benzenes<sup>17,18</sup> were calculated using wave functions obtained from the CNDO procedure. The calculated results were in good agreement with the experimental data not only for  $\pi^* \leftarrow \pi$  transitions,<sup>10,11,13,15-18</sup> but also for  $\pi^* \leftarrow n$  transitions.<sup>12,14,16,18</sup> The magnetic mixing of the  $\pi^* \leftarrow \sigma$  and the  $\pi^* \leftarrow n$  states with the  $\pi^* \leftarrow \pi$  state was found to be of importance in the lowest  $\pi^* \leftarrow \pi$  transition of indole,<sup>15</sup> pyridazine,<sup>16</sup> and pyrimidine.<sup>16</sup>

In this work, we measure the MCD spectra of quinoline, isoquinoline, quinoxaline, phthalazine, quinazoline, cinnoline,

and pyrido[2,3-*b*]pyrazine, and calculate the Faraday *B* terms of these azanaphthalenes using CNDO/S-CI method.<sup>9</sup> We also examine the spectral assignment of azanaphthalenes and elucidate the origins for the Faraday *B* terms of two lowest  $\pi^* \leftarrow \pi$  transitions and the lowest allowed  $\pi^* \leftarrow n$  transition of azanaphthalenes.

## Experimental Section

Quinoline, isoquinoline, and quinoxaline were distilled under reduced pressure. Phthalazine, quinazoline, and pyrido[2,3-*b*]pyrazine were purified by recrystallization from ether, petroleum ether, and ethanol-petroleum ether, respectively. Cinnoline was sublimed under reduced pressure just before the measurements. Spectrograde *n*-heptane was used as a solvent.

The MCD spectra were recorded with a JASCO J-20A recording circular dichrometer equipped with a 11.4-kG electromagnet. The absorption spectra were measured on a Hitachi EPS-3T recording spectrophotometer.

The experimental values of the Faraday *B* terms were obtained from the MCD spectra by use of the method of moments,<sup>19</sup> after the overlapping bands were separated by the Gaussian curve fitting procedure.

## Theoretical Section

Transition energies, oscillator strengths, and Faraday *B* terms were calculated using wave functions obtained from the CNDO/S-CI method.<sup>9</sup> Configuration interactions (CI) among singly excited configurations below 10 eV (60–70 configurations) were taken into account. The parameters of the CNDO/S-CI method were reported previously.<sup>16</sup> The bond lengths and bond angles were taken from the experimental values of benzene and azabenzene.<sup>20</sup>

The Faraday *B* term of a transition from the ground state *a* to the excited state *j* is given by<sup>19,21</sup>

$$B(j \leftarrow a) = \sum_{k \neq a,j} B_{j,k} + \sum_{k \neq a,j} B_{k,a} + B_{j,a} \quad (1)$$

where

$$B_{j,k} = \text{Im} \langle j | \boldsymbol{\mu} | k \rangle \cdot \langle a | \mathbf{M} | j \rangle \times \langle k | \mathbf{M} | a \rangle / (E_k - E_j) \quad (2)$$

$$B_{k,a} = \text{Im} \langle k | \boldsymbol{\mu} | a \rangle \cdot \langle a | \mathbf{M} | j \rangle \times \langle j | \mathbf{M} | k \rangle / (E_k - E_a) \quad (3)$$

$$B_{j,a} = \text{Im} \langle j | \boldsymbol{\mu} | a \rangle \cdot \langle a | \mathbf{M} | j \rangle \times (\langle j | \mathbf{M} | j \rangle - \langle a | \mathbf{M} | a \rangle) / (E_j - E_a) \quad (4)$$

In eq 2–4,  $E_a$ ,  $E_j$ , and  $E_k$  are the energies of the states *a*, *j*, and *k*, respectively, and  $\mathbf{M}$  and  $\boldsymbol{\mu}$  are the electric and magnetic moment operators, respectively.  $B_{j,k}$  stands for the magnetic mixing of the state *k* with the excited state *j*, and  $B_{k,a}$  represents the coupling of the state *k* to the ground state *a*.  $B_{j,a}$  arises

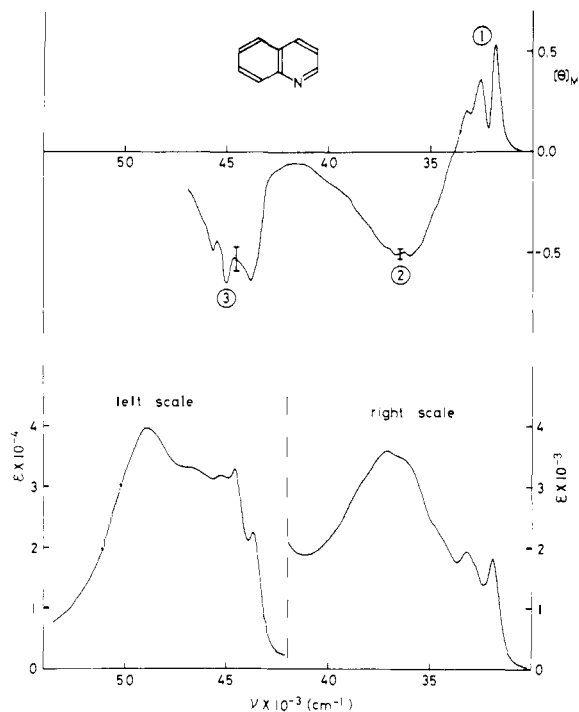


Figure 1. MCD (upper) and absorption (lower) spectra of quinoline in *n*-heptane solution at room temperature.

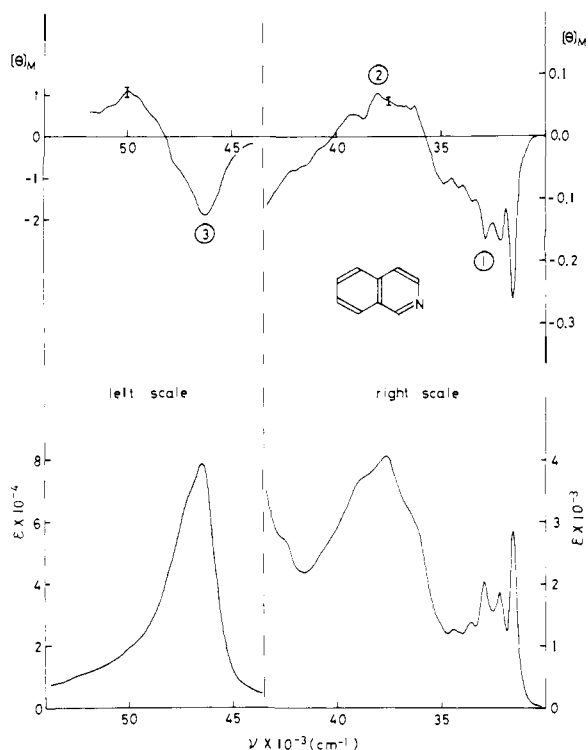


Figure 2. MCD (upper) and absorption (lower) spectra of isoquinoline in *n*-heptane solution at room temperature.

from the magnetic mixing between the ground state *a* and the excited state *j*.

The electric transition moments were evaluated by the dipole length operator. The LCAO-MO coefficients regarding the orthogonalized CNDO atomic orbital basis were deorthogonalized by the inverse Löwdin transformation<sup>22</sup> and atomic integrals were calculated using Slater atomic orbitals<sup>23</sup> in accordance with the description of ref 24 and 25.

The Faraday *B* terms calculated for noncentric molecules using a limited basis set linearly depend on the origin.<sup>26,27</sup> In

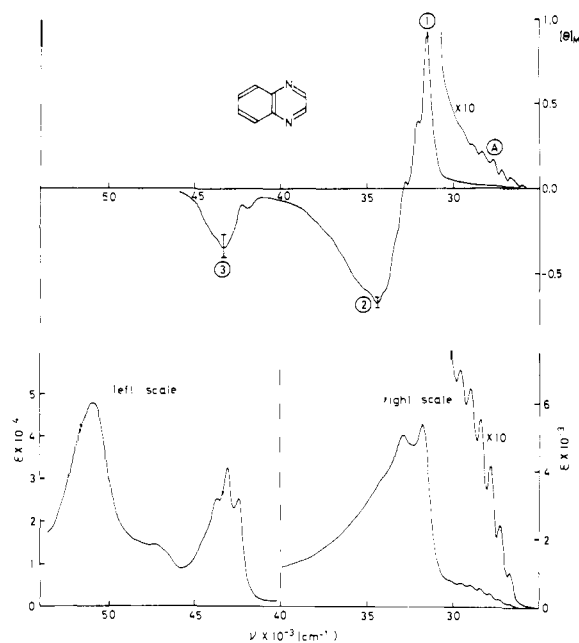


Figure 3. MCD (upper) and absorption (lower) spectra of quinoxaline in *n*-heptane solution at room temperature.

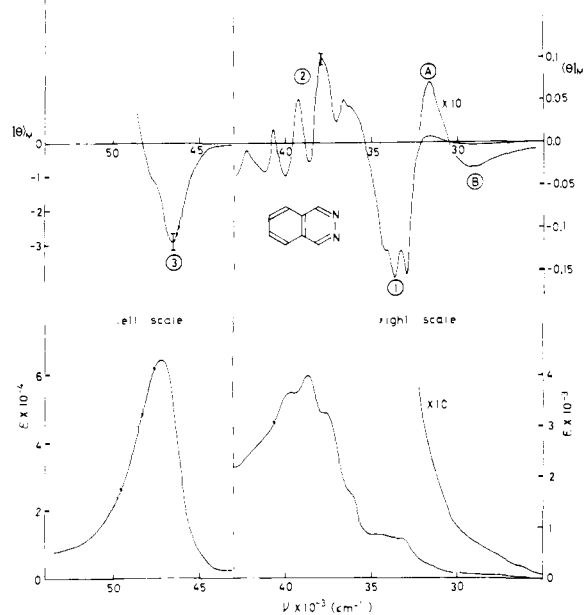


Figure 4. MCD (upper) and absorption (lower) spectra of phthalazine in *n*-heptane solution at room temperature.

this work, the origin was chosen at the center of the electron cloud in the ground state according to the theoretical argument of Caldwell and Eyring.<sup>27</sup> The degree of the origin dependence of the calculated *B* terms was also investigated.

Calculations were carried out using an ACOS 700 computer in the computer center of Tohoku University.

## Results and Discussion

**Experimental Results.** The MCD and absorption spectra of azanaphthalenes are shown in Figures 1–7. The molar ellipticity per unit magnetic field,  $[\theta]_M$ , and the extinction coefficient,  $\epsilon$ , are expressed in degree deciliter mole<sup>-1</sup> decimeter<sup>-1</sup> gauss<sup>-1</sup> and in liter mole<sup>-1</sup> cm<sup>-1</sup> units, respectively.

In the lower wavenumber region (22 000–32 000 cm<sup>-1</sup>), quinoxaline, phthalazine, quinazoline, and cinnoline show a positive MCD band (band A), while quinoline and isoquinoline

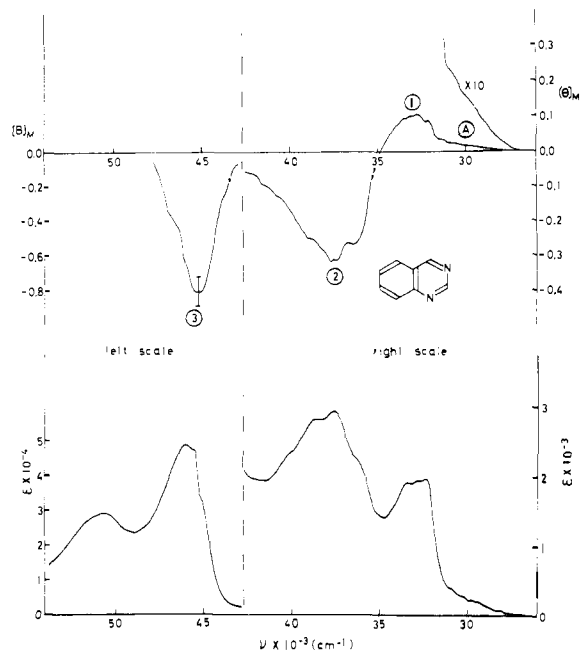


Figure 5. MCD (upper) and absorption (lower) spectra of quinazoline in *n*-heptane solution at room temperature.

exhibit no MCD and absorption band in this spectral region. No distinct MCD is observed for band A pyrido[2,3-*b*]pyrazine. In the case of phthalazine, a negative MCD band (band B) is observed at lower wavenumber than band A (Figure 4).

In the middle wavenumber region (30 000–43 000  $\text{cm}^{-1}$ ), we can identify two MCD bands with opposite sign (bands 1 and 2) which are overlapping with each other in the absorption spectrum. The vibrational structure with a progression in a 600–700- $\text{cm}^{-1}$  vibration is observed in the MCD and absorption spectra of band 1 of quinoline, isoquinoline, quinoxaline, phthalazine, and pyrido[2,3-*b*]pyrazine. Band 2 of phthalazine also shows the complicated MCD spectrum consisting of two vibrational progressions with opposite sign in an about 1500- $\text{cm}^{-1}$  vibration (Figure 4). The signs and the magnitudes of the MCD of bands 1 and 2 are closely related to the position at which the aza substitution occurs. In the case of quinoline and quinoxaline, which contain nitrogen atoms at the  $\alpha$  position, the positive and negative MCD bands are observed for bands 1 and 2, respectively. On the contrary,  $\beta$ -azanaphthalenes, such as isoquinoline and phthalazine, show negative and positive MCD bands for bands 1 and 2, respectively. The MCD spectra of bands 1 and 2 of  $\alpha,\beta$ -diazanaphthalenes (quinazoline and cinnoline) are similar in sign to those of quinoline and quinoxaline, but smaller in magnitude than the MCD of these  $\alpha$ -azanaphthalenes.

In the higher wavenumber region (42 000–53 000  $\text{cm}^{-1}$ ), the intense absorption bands ( $\epsilon \approx 10^4$ – $10^5$ ) are observed. Each compound show a negative MCD band (band 3) in the wavenumber region of 42 000–48 000  $\text{cm}^{-1}$ , but the MCD spectrum in the region higher than 48 000  $\text{cm}^{-1}$  is not clearly measured because of the poor signal to noise ratio.

**Spectral Assignments and Calculated Results.** The observed and calculated transition energies, oscillator strengths, and Faraday *B* terms are presented in Tables I–III. Several weak  $\pi^* \leftarrow \sigma$  and  $\sigma^* \leftarrow \pi$  transitions predicted in the region higher than 40 000  $\text{cm}^{-1}$  are omitted from Tables I–III.

The absorption spectrum of diazanaphthalenes in the lower wavenumber region (22 000–32 000  $\text{cm}^{-1}$ ) has been extensively studied.<sup>28–32</sup> Band A of quinoxaline was assigned to the symmetry allowed  ${}^1B_1 \leftarrow {}^1A_1$  ( $\pi^* \leftarrow n$ ) transition.<sup>28</sup> Band A of

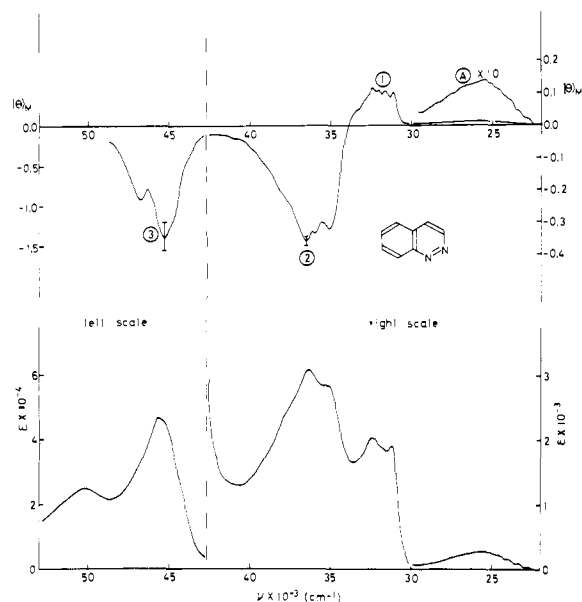


Figure 6. MCD (upper) and absorption (lower) spectra of cinnoline in *n*-heptane solution at room temperature.

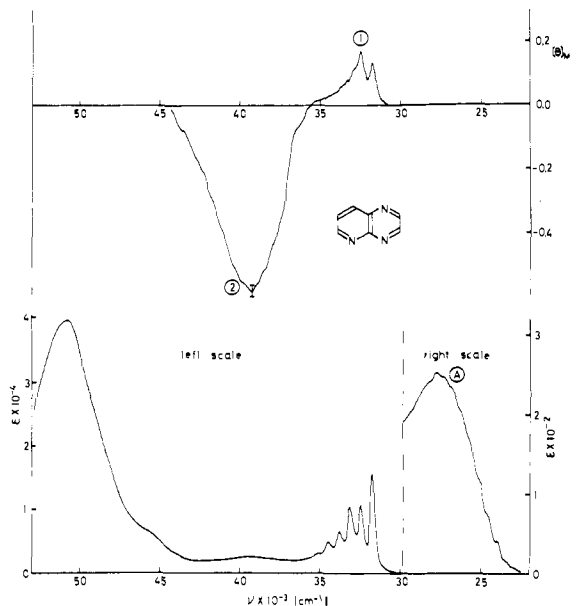


Figure 7. MCD (upper) and absorption (lower) spectra of pyrido[2,3-*b*]pyrazine in *n*-heptane solution at room temperature.

quinazoline and cinnoline was also attributed to the lowest  $\pi^* \leftarrow n$  transition.<sup>29,30</sup> The results of the present calculations are in coincidence with these assignments.

On the other hand, the spectral assignment of the  $\pi^* \leftarrow n$  transitions of phthalazine has been a subject of considerable debate. On the basis of the analysis of the vibrational structure of the crystalline spectrum, Hochstrasser and Marzacco<sup>31</sup> first reported that the lowest absorption band (25 000–29 000  $\text{cm}^{-1}$ ) of phthalazine consists of two independent  $\pi^* \leftarrow n$  transitions with  ${}^1A_2 \leftarrow {}^1A_1$  symmetry. Then, Hochstrasser and Wiersma<sup>32</sup> measured the permanent dipole moment changes, associated with vibronic transitions in this spectral region, aiming at obtaining more detailed information on the spectral assignment. From the result that the values of dipole moment changes are equal ( $3.05 \pm 0.10$  D) for all vibronic transitions, they revised the assignment and concluded that there is only one  ${}^1A_2 \leftarrow {}^1A_1$  ( $\pi^* \leftarrow n$ ) transition in this spectral region. The present CNDO/S-CI calculation predicts the  ${}^1A_2 \leftarrow {}^1A_1$

Table I. Experimental and Calculated Results for  $\alpha$ -Azanaphthalenes

Compd	Band	$\nu_{\text{obsd}} \times 10^{-3}$ , cm <sup>-1</sup>	$\nu_{\text{calcd}} \times 10^{-3}$ , cm <sup>-1</sup>	$f_{\text{obsd}}$	$f_{\text{calcd}}$	$B_{\text{obsd}} \times 10^4$ , $\beta D^2$ cm	$B_{\text{calcd}} \times 10^4$ , $\beta D^2$ cm	Assignment	
Quinoline	1	32.4	32.7	0.009	0.015	-9.0	-21.1	$\pi^* \leftarrow \pi$ <sup>1</sup> A'	
			33.3		0.003		-2.6	$\pi^* \leftarrow n$ <sup>1</sup> A''	
	2	36.6	35.2	0.083	0.187	21	32.9	$\pi^* \leftarrow \pi$ <sup>1</sup> A'	
		3	45.0		44.4		1.055	13	27.2
				45.9	0.034		-34.6	$\pi^* \leftarrow \pi$ <sup>1</sup> A'	
			49.0	47.6	1.20	0.813	2.0	$\pi^* \leftarrow \pi$ <sup>1</sup> A'	
			50.2	0.529		-2.7	$\pi^* \leftarrow \pi$ <sup>1</sup> A'		
Quinoxaline	A	28.9	26.6	0.004	0.003	-1 to -2	-1.31	$\pi^* \leftarrow n$ <sup>1</sup> B <sub>1</sub>	
	1	32.3	32.2	0.024	0.107	-16	-93.7	$\pi^* \leftarrow \pi$ <sup>1</sup> A <sub>1</sub>	
		2	35.0	33.5	0.093		0.142	23	109
				39.2		Forbidden	Forbidden	$\pi^* \leftarrow \sigma$ <sup>1</sup> A <sub>2</sub>	
	3	43.2	43.1	0.29	0.784	5.7	13.7	$\pi^* \leftarrow \pi$ <sup>1</sup> A <sub>1</sub>	
			47.1	46.6	0.20		0.010	-21.7	$\pi^* \leftarrow \pi$ <sup>1</sup> B <sub>2</sub>
			51.1	49.0	0.61	0.961	-54.1	$\pi^* \leftarrow \pi$ <sup>1</sup> A <sub>1</sub>	
				50.6	0.543		48.8	$\pi^* \leftarrow \pi$ <sup>1</sup> B <sub>2</sub>	
Pyrido[2.3- <i>b</i> ]pyrazine	A	26.4	25.3	0.003	0.001	0.0	-0.4	$\pi^* \leftarrow n$ <sup>1</sup> A''	
	1	32.6	31.8	0.096	0.255	-2.6	-32.7	$\pi^* \leftarrow \pi$ <sup>1</sup> A'	
				33.9	0.006		-4.0	$\pi^* \leftarrow n$ <sup>1</sup> A''	
	2	38.6	36.7	38.7	0.062	0.162	20	61.7	$\pi^* \leftarrow \pi$ <sup>1</sup> A'
				38.7		0.000		0.0	$\pi^* \leftarrow n$ <sup>1</sup> A''
			44.6	48.2		0.164		-2.6	$\pi^* \leftarrow \pi$ <sup>1</sup> A'
				48.2		0.237		35.6	$\pi^* \leftarrow \pi$ <sup>1</sup> A'
			50.1	48.8	0.87	1.356		-121	$\pi^* \leftarrow \pi$ <sup>1</sup> A'
			50.0		0.492		68.3	$\pi^* \leftarrow \pi$ <sup>1</sup> A'	

Table II. Experimental and Calculated Results for  $\beta$ -Azanaphthalenes

Compd	Band	$\nu_{\text{obsd}} \times 10^{-3}$ , cm <sup>-1</sup>	$\nu_{\text{calcd}} \times 10^{-3}$ , cm <sup>-1</sup>	$f_{\text{obsd}}$	$f_{\text{calcd}}$	$B_{\text{obsd}} \times 10^4$ , $\beta D^2$ cm	$B_{\text{calcd}} \times 10^4$ , $\beta D^2$ cm	Assignment	
Isoquinoline	1	32.3	31.8	0.017	0.100	4.7	27.7	$\pi^* \leftarrow \pi$ <sup>1</sup> A'	
			33.8		0.002		-0.12	$\pi^* \leftarrow n$ <sup>1</sup> A''	
	2	38.8	35.5	0.110	0.170	Negative	-37.4	$\pi^* \leftarrow \pi$ <sup>1</sup> A'	
			44.3		0.161		-2.5	$\pi^* \leftarrow \pi$ <sup>1</sup> A'	
	3	46.7	46.7	1.2	1.713	34	191	$\pi^* \leftarrow \pi$ <sup>1</sup> A'	
			49.5		47.7		0.031	-23	-163
			51.1	0.470		8.1	$\pi^* \leftarrow \pi$ <sup>1</sup> A'		
Phthalazine	B	29.1	34.8		Forbidden	0.1	Forbidden	$\pi^* \leftarrow n$ <sup>1</sup> A <sub>2</sub>	
	A	31.6	32.9	0.003	0.006	-0.3	-7.79	$\pi^* \leftarrow n$ <sup>1</sup> B <sub>1</sub>	
	1	33.3	33.3	0.004	0.072	2.6	49.4	$\pi^* \leftarrow \pi$ <sup>1</sup> A <sub>1</sub>	
		2	39.2	36.1	0.094		0.196	Negative	-56.4
				41.9	0.000		0.0		$\pi^* \leftarrow \sigma$ <sup>1</sup> B <sub>1</sub>
			43.1		Forbidden		Forbidden	$\pi^* \leftarrow \sigma$ <sup>1</sup> A <sub>2</sub>	
			46.7		1.065		-37.1	$\pi^* \leftarrow \pi$ <sup>1</sup> A <sub>1</sub>	
	3	47.1	47.0	47.0	1.07	0.005	30	77.3	$\pi^* \leftarrow \pi$ <sup>1</sup> B <sub>2</sub>
				48.2		0.812		54.1	$\pi^* \leftarrow \pi$ <sup>1</sup> A <sub>1</sub>
				50.3		0.553		-52.3	$\pi^* \leftarrow \pi$ <sup>1</sup> B <sub>2</sub>

( $\pi^* \leftarrow n$ ) and <sup>1</sup>B<sub>1</sub> ← <sup>1</sup>A<sub>1</sub> ( $\pi^* \leftarrow n$ ) transitions at 34 800 and 32 900 cm<sup>-1</sup>, respectively. Since the second <sup>1</sup>A<sub>2</sub> ← <sup>1</sup>A<sub>1</sub> ( $\pi^* \leftarrow n$ ) transition is calculated at higher wavenumber (43 100 cm<sup>-1</sup>), band B of phthalazine is considered to contain only the lowest <sup>1</sup>A<sub>2</sub> ← <sup>1</sup>A<sub>1</sub> ( $\pi^* \leftarrow n$ ) transition. At 31 600 cm<sup>-1</sup>, we can identify a positive MCD band (band A), which is assignable to the symmetry allowed <sup>1</sup>B<sub>1</sub> ← <sup>1</sup>A<sub>1</sub> ( $\pi^* \leftarrow n$ ) transition.

From the comparison between the experimental and calculated results, bands 1 and 2 in azanaphthalenes can be attributed to the first and second  $\pi^* \leftarrow \pi$  transitions, respectively. However, the situation for band 2 of phthalazine is more complicated. Within this band, we observed sign alternations of the MCD spectrum (Figure 4), for which the following two interpretations may be alternatively considered. First, band 2 of phthalazine consists of only the second  $\pi^* \leftarrow \pi$  transition whose vibronic components show oppositely signed MCD to each other. In this case, the MCD is considered to be dominated not only by symmetry-allowed transition moments, but

also by vibronically induced ones. Secondly, band 2 of phthalazine is composed of at least two independent electronic transitions. In addition to the second  $\pi^* \leftarrow \pi$  transitions, two  $\pi^* \leftarrow \sigma$  transitions calculated at 41 900 and 43 100 cm<sup>-1</sup> (Table II) are expected to lie in this spectral region.

Although four  $\pi^* \leftarrow \pi$  transitions are calculated in the higher wavenumber region (42 000–53 000 cm<sup>-1</sup>), the detailed assignment in this spectral region could not be achieved because the MCD and absorption bands are poorly resolved.

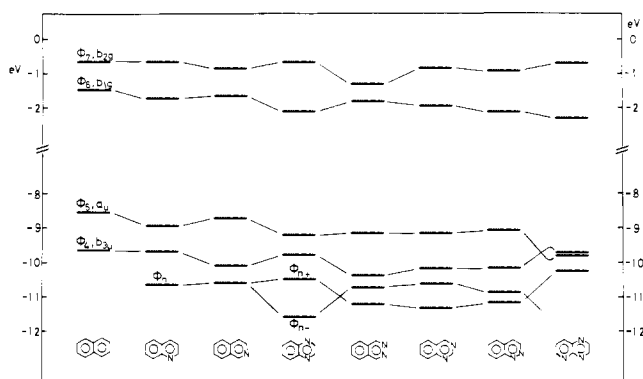
As the calculated order of the lowest  $\pi^* \leftarrow n$  and the lowest  $\pi^* \leftarrow \pi$  states of quinazoline is incorrect, the calculated signs of the Faraday *B* terms of the lowest  $\pi^* \leftarrow n$  and  $\pi^* \leftarrow \pi$  transitions of quinazoline are considered to be unreliable. Therefore, we also calculated the magnetic mixing between these excited states using the experimental transition energies for the energy difference denominator in eq 2 and showed the corrected *B* terms in parentheses in Table III.

Although the present CNDO/S-CI calculation gave an

**Table III.** Experimental and Calculated Results for  $\alpha,\beta$ -Diazanaphthalenes

Compd	Band	$\nu_{\text{obsd}} \times 10^{-3}$ , cm <sup>-1</sup>	$\nu_{\text{calcd}} \times 10^{-3}$ , cm <sup>-1</sup>	$f_{\text{obsd}}$	$f_{\text{calcd}}$	$B_{\text{obsd}} \times 10^4$ , $\beta D^2$ cm	$B_{\text{calcd}} \times 10^4$ , $\beta D^2$ cm	Assignment		
Quinoxaline	A	29.5	32.6	0.002	0.003	-0.3	8.4 (-2.1) <sup>a</sup>	$\pi^* \leftarrow n$ <sup>1</sup> A''		
	1	32.9	32.5	0.018	0.091	-3.6	-12.3 (-1.8) <sup>a</sup>	$\pi^* \leftarrow \pi$ <sup>1</sup> A'		
	2	38.4		36.2	0.078	0.101	12	5.6	$\pi^* \leftarrow \pi$ <sup>1</sup> A'	
				38.0		0.000		0.4		$\pi^* \leftarrow n$ <sup>1</sup> A''
	3	46.1	50.2	45.5	0.56	0.917	14	28.2	$\pi^* \leftarrow \pi$ <sup>1</sup> A'	
				46.1		0.587		-21.7		$\pi^* \leftarrow \pi$ <sup>1</sup> A'
				48.8	0.60	0.375		-5.3		$\pi^* \leftarrow \pi$ <sup>1</sup> A'
			51.8		0.415		4.5	$\pi^* \leftarrow \pi$ <sup>1</sup> A'		
Cinnoline	A	25.9	28.5	0.005	0.004	-0.7	-2.2	$\pi^* \leftarrow n$ <sup>1</sup> A''		
	1	31.9	31.7	0.016	0.107	-4.2	-3.6	$\pi^* \leftarrow \pi$ <sup>1</sup> A'		
	2	36.6		34.3	0.080	0.107	14	7.7	$\pi^* \leftarrow \pi$ <sup>1</sup> A'	
				35.9		0.000		0.1		$\pi^* \leftarrow n$ <sup>1</sup> A''
	3	45.5	49.7	45.0	0.54	1.207	13	66.7	$\pi^* \leftarrow \pi$ <sup>1</sup> A'	
				45.5		0.102		-67.4		$\pi^* \leftarrow \pi$ <sup>1</sup> A'
				47.8	0.61	0.672		5.9		$\pi^* \leftarrow \pi$ <sup>1</sup> A'
			50.6		0.234		2.8	$\pi^* \leftarrow \pi$ <sup>1</sup> A'		

<sup>a</sup> The magnetic mixing between the lowest  $\pi^* \leftarrow n$  and the lowest  $\pi^* \leftarrow \pi$  states was evaluated using experimental transition energies for the denominator of eq 2.

**Figure 8.** Calculated molecular orbital energies of azanaphthalenes.

incorrect order of the low-lying states of phthalazine and quinoxaline, the calculated transition energies agree fairly well with the experimental data. The calculated magnitudes of oscillator strengths and Faraday  $B$  terms tend to be larger than the experimental ones, as usual in the dipole length method. However, the calculated signs of the Faraday  $B$  terms are in perfect agreement with the experimental results.

**Origin Dependence of the Calculated  $B$  Terms.** The Faraday  $B$  terms calculated for noncentric molecules using a limited basis set linearly depend on the origin. We have also calculated the Faraday  $B$  terms at the point 1 Å from the center of charge in the ground state and shown the results for quinoxaline and phthalazine in Table IV. The origin dependence of the calculated  $B$  terms is so small that the sign and the order of the theoretical  $B$  terms are not significantly changed as long as the origin is transformed within the molecular framework.

**Molecular Orbitals and Electronic States.** Two HOMOs ( $\phi_4$  and  $\phi_5$ ), two LUMOs ( $\phi_6$  and  $\phi_7$ ), and the nitrogen lone pair orbitals ( $\phi_n$ ) are shown in Figure 8. The lone pair orbitals in diazanaphthalenes and triazanaphthalenes are split by the through-bond interaction, and can be classified approximately as symmetric combination ( $\phi_{n+}$ ) and antisymmetric combination ( $\phi_{n-}$ ) of the nitrogen lone pair orbitals. In the cases of phthalazine, quinoxaline, and cinnoline, the MO  $\phi_{n-}$  lies higher than the MO  $\phi_{n+}$ , while the order of these lone pair orbitals of quinoxaline and pyrido[2,3-*b*]pyrazine is opposite to this.

The energies of  $\pi$  MOs are considerably affected by aza substitutions.  $\alpha$ -Aza substitution lowers the MOs  $\phi_5$  and  $\phi_6$ ,

**Table IV.** Calculated Faraday  $B$  Terms of Quinoxaline and Phthalazine at the Point 1 Å Away from the Center of the Electron Cloud along the  $C_2$  Axis of the Molecules

Compd	$\nu_{\text{calcd}} \times 10^{-3}$ , cm <sup>-1</sup>	$B_{\text{calcd}} \times 10^4$ , $\beta D^2$ cm	Assignment
Quinoxaline	26.6	-1.30	$\pi^* \leftarrow n$ <sup>1</sup> B <sub>1</sub>
	32.2	-93.8	$\pi^* \leftarrow \pi$ <sup>1</sup> A <sub>1</sub>
	33.5	111	$\pi^* \leftarrow \pi$ <sup>1</sup> B <sub>2</sub>
	43.1	13.3	$\pi^* \leftarrow \pi$ <sup>1</sup> A <sub>1</sub>
	46.6	-22.2	$\pi^* \leftarrow \pi$ <sup>1</sup> B <sub>2</sub>
	49.0	-67.1	$\pi^* \leftarrow \pi$ <sup>1</sup> A <sub>1</sub>
	50.6	62.4	$\pi^* \leftarrow \pi$ <sup>1</sup> B <sub>2</sub>
Phthalazine	32.9	-5.82	$\pi^* \leftarrow n$ <sup>1</sup> B <sub>1</sub>
	33.3	48.0	$\pi^* \leftarrow \pi$ <sup>1</sup> A <sub>1</sub>
	36.1	-56.2	$\pi^* \leftarrow \pi$ <sup>1</sup> B <sub>2</sub>
	46.7	-47.2	$\pi^* \leftarrow \pi$ <sup>1</sup> A <sub>1</sub>
	47.0	83.2	$\pi^* \leftarrow \pi$ <sup>1</sup> B <sub>2</sub>
	48.2	47.7	$\pi^* \leftarrow \pi$ <sup>1</sup> A <sub>1</sub>
	50.3	-53.8	$\pi^* \leftarrow \pi$ <sup>1</sup> B <sub>2</sub>

relative to naphthalene, whereas the MOs  $\phi_4$  and  $\phi_7$  are insensitive to the  $\alpha$ -aza substitution. Contrary to this,  $\beta$ -aza substitution lowers the MOs  $\phi_4$  and  $\phi_7$  more effectively than the MOs  $\phi_5$  and  $\phi_6$ .

Let us first consider the electronic states of naphthalene itself. One-electron jumps from the MOs  $\phi_4$  ( $b_{3u}$ ) and  $\phi_5$  ( $a_u$ ) to the MOs  $\phi_6$  ( $b_{1g}$ ) and  $\phi_7$  ( $b_{2g}$ ) give rise to four  $\pi^* \leftarrow \pi$  states with <sup>1</sup>B<sub>2u</sub> and <sup>1</sup>B<sub>1u</sub> symmetries,<sup>33</sup> which are named as <sup>1</sup>L<sub>b</sub> (<sup>1</sup>B<sub>2u</sub>), <sup>1</sup>L<sub>a</sub> (<sup>1</sup>B<sub>1u</sub>), <sup>1</sup>B<sub>b</sub> (<sup>1</sup>B<sub>2u</sub>), and <sup>1</sup>B<sub>a</sub> (<sup>1</sup>B<sub>1u</sub>), in the order of increasing energy, in the Platt nomenclature system.<sup>34</sup> The <sup>1</sup>L<sub>b</sub> and <sup>1</sup>B<sub>b</sub> states are expressed as antisymmetric and symmetric combinations, respectively, of the configurations  $\psi_{4 \rightarrow 6}$  and  $\psi_{5 \rightarrow 7}$ . On the other hand, the <sup>1</sup>L<sub>a</sub> state can be approximated by a single configuration,  $\psi_{5 \rightarrow 6}$ , and the <sup>1</sup>B<sub>a</sub> state by  $\psi_{4 \rightarrow 7}$ . In addition, two symmetry-forbidden transitions from the ground state to the <sup>1</sup>B<sub>3g</sub> ( $\psi_{5 \rightarrow 8}$ ) and <sup>1</sup>A<sub>g</sub> ( $\psi_{3 \rightarrow 7}$ ,  $\psi_{4 \rightarrow 8}$ ,  $\psi_{5 \rightarrow 9}$ ) states are also predicted in the ultraviolet region.

Then, we consider the electronic states of azanaphthalenes. As seen from the wave functions given in the Appendix, the first and the second  $\pi^* \leftarrow \pi$  states of quinoline, quinoxaline, phthalazine, and pyrido[2,3-*b*]pyrazine approximately correspond to the <sup>1</sup>L<sub>b</sub> ( $(\psi_{4 \rightarrow 6} - \psi_{5 \rightarrow 7})/\sqrt{2}$ ) and <sup>1</sup>L<sub>a</sub> ( $\psi_{5 \rightarrow 6}$ ) states, respectively, whereas two lowest  $\pi^* \leftarrow \pi$  states of isoquinoline, quinoxaline, and cinnoline are regarded as the mixture of the <sup>1</sup>L<sub>b</sub> and <sup>1</sup>L<sub>a</sub> states. The third-sixth  $\pi^* \leftarrow \pi$  states of aza-

**Table V.** Contribution to the Faraday  $B$  Terms ( $\beta D^2$  cm) of Two Lowest  $\pi^* \leftarrow \pi$  Transitions from Each Excited State

Compd	State $j$	$B_{j,k} \times 10^4$ for state $k =$						1st $\pi^* \leftarrow \pi$	2nd $\pi^* \leftarrow \pi$
		1st $\pi^* \leftarrow \pi$	2nd $\pi^* \leftarrow \pi$	3rd $\pi^* \leftarrow \pi$	4th $\pi^* \leftarrow \pi$	5th $\pi^* \leftarrow \pi$	6th $\pi^* \leftarrow \pi$		
Quinoline	1st $\pi^* \leftarrow \pi$		-23.7	0.1	0.0	-0.2	2.8	0.2	
	2nd $\pi^* \leftarrow \pi$	23.7		2.9	0.2	3.9	0.1	2.0	
Isoquinoline	1st $\pi^* \leftarrow \pi$		31.6	0.3	-1.8	-0.1	-2.7	0.0	
	2nd $\pi^* \leftarrow \pi$	-31.6		-1.2	-2.6	-0.3	-1.9	-0.8	
Quinoxaline	1st $\pi^* \leftarrow \pi$		-98.0	-1.2	0.0	0.0	7.2	0.0	0.0
	2nd $\pi^* \leftarrow \pi$	98.0		0.0	5.5	5.6	0.0	0.7	0.0
Phthalazine	1st $\pi^* \leftarrow \pi$		49.3	0.0	0.2	0.0	-6.5	0.0	6.2
	2nd $\pi^* \leftarrow \pi$	-49.3		-3.3	0.0	-3.8	0.0	0.0	-0.4
Quinazoline	1st $\pi^* \leftarrow \pi$		-4.3	-0.8	4.7	-0.6	-0.9	0.5 <sup>a</sup>	0.0
	2nd $\pi^* \leftarrow \pi$	4.3		1.2	-2.3	0.6	1.7	0.4	-0.2
Cinnoline	1st $\pi^* \leftarrow \pi$		-6.5	3.8	-1.8	0.7	-0.2	0.8	0.0
	2nd $\pi^* \leftarrow \pi$	6.5		-2.9	1.9	0.7	0.5	0.1	0.1
Pyrido[2,3- <i>b</i> ]pyrazine	1st $\pi^* \leftarrow \pi$		-43.1	-0.1	3.8	-0.1	8.1	0.0	1.0
	2nd $\pi^* \leftarrow \pi$	43.1		2.8	0.6	13.5	.0	0.1	2.1

<sup>a</sup> This value was calculated using the experimental transition energies for the denominator of eq 2.

**Table VI.** Contribution to the Faraday  $B$  Term ( $\beta D^2$  cm) of the Lowest Allowed  $\pi^* \leftarrow n$  Transition from Electronic States

Compd	$B_{j,k} \times 10^4$ for state $k =$				$(\sum_k^{\sigma} B_{k,a} + B_{j,a}) \times 10^4$
	1st $\pi^* \leftarrow \pi$	2nd $\pi^* \leftarrow \pi$	3rd $\pi^* \leftarrow \pi$	4th $\pi^* \leftarrow \pi$	
Quinoline	-0.18	-2.03	0.10	0.01	-0.27
Isoquinoline	0.02	0.76	-0.05	-0.37	-0.30
Quinoxaline	0.01	-0.70	0.01	0.0	-0.56
Phthalazine	-6.17	0.35	-0.83	0.0	-0.81
Quinazoline	-0.47 <sup>a</sup>	-0.38	-0.29	-0.15	-0.56
Cinnoline	-0.84	-0.14	-0.35	-0.04	-0.64
Pyrido[2,3- <i>b</i> ]pyrazine	0.04	-0.14	0.02	-0.07	-0.24

<sup>a</sup> This value was calculated using the experimental transition energies for the denominator of eq 2.

naphthalenes are composed of the electronic configurations  $\psi_{3 \rightarrow 6}$ ,  $\psi_{4 \rightarrow 6}$ ,  $\psi_{4 \rightarrow 7}$ ,  $\psi_{4 \rightarrow 8}$ ,  $\psi_{5 \rightarrow 7}$ ,  $\psi_{5 \rightarrow 8}$ , and  $\psi_{5 \rightarrow 9}$ , which considerably mix with each other by the configuration interactions. It seems to be difficult to correlate these higher excited states of azanaphthalenes with the electronic states of naphthalene itself.

**Origin for the Faraday  $B$  Terms of Two Lowest  $\pi^* \leftarrow \pi$  Transitions.** The calculated results show that the main part of the Faraday  $B$  terms of the  $\pi^* \leftarrow \pi$  transitions is induced by the magnetic mixing among  $\pi^* \leftarrow \pi$  states, the first term of eq 1. The contributions to the  $B$  terms of two lowest  $\pi^* \leftarrow \pi$  transitions from each  $\pi^* \leftarrow \pi$  state are given in Table V. The Faraday  $B$  terms of two lowest  $\pi^* \leftarrow \pi$  transitions can be interpreted as mainly arising from the mutual mixing of two lowest  $\pi^* \leftarrow \pi$  states leading to opposite sign of the Faraday  $B$  terms of these transitions. The magnetic mixing of the  $\pi^* \leftarrow n$  state with the  $\pi^* \leftarrow \pi$  state is not of much importance in the  $B$  terms of the  $\pi^* \leftarrow \pi$  transitions of azanaphthalenes.

Let us try to explain the sign of the magnetic mixing of two lowest  $\pi^* \leftarrow \pi$  states on the basis of the theoretical argument proposed by Michl.<sup>6,35</sup> As shown in the Appendix, the lowest ( $\psi_1$ ) and the second ( $\psi_2$ )  $\pi^* \leftarrow \pi$  states of azanaphthalenes are approximately expressed as linear combinations of the configurations  $\psi_{4 \rightarrow 6}$ ,  $\psi_{5 \rightarrow 7}$ , and  $\psi_{5 \rightarrow 6}$ , namely,

$$\psi_1 = C_1\psi_{4 \rightarrow 6} - C_2\psi_{5 \rightarrow 7} + C_3\psi_{5 \rightarrow 6} \quad (5)$$

$$\psi_2 = C_4\psi_{4 \rightarrow 6} - C_5\psi_{5 \rightarrow 7} - C_6\psi_{5 \rightarrow 6} \quad (6)$$

where the coefficients  $C_1$ - $C_6$ , are taken to be positive. For quinoxaline and phthalazine, which belong to  $C_{2v}$  point group,  $C_3$ ,  $C_4$ , and  $C_5$  are zero.

Between molecular integrals of the electric and magnetic moment operators, the following relations are obtained using alternant pairing properties.<sup>35</sup>

$$\langle \phi_4 | m_y | \phi_6 \rangle \approx \langle \phi_5 | m_y | \phi_7 \rangle \equiv m_y \quad (7)$$

$$\langle \phi_5 | m_z | \phi_6 \rangle \equiv m_z \quad (8)$$

$$\text{Im} \langle \phi_6 | l_x | \phi_7 \rangle \approx \text{Im} \langle \phi_4 | l_x | \phi_5 \rangle \equiv l_x \quad (9)$$

where  $m_y$  and  $m_z$  are the  $y$  and  $z$  components<sup>33</sup> of the one-electron operator of the electric moments, and  $l_x$  is the  $x$  component<sup>33</sup> of the one-electron operator of the orbital angular momentum. Since the LCAO-MO coefficients in the MOs  $\phi_4$ - $\phi_7$  are relatively insensitive to the aza substitution, eq 7-9 also approximately hold for azanaphthalenes. From eq 5-9, the electric and magnetic transition moments among ground state,  $\psi_0$ , and excited states,  $\psi_1$  and  $\psi_2$ , are expressed as

$$\langle \phi_0 | M | \psi_1 \rangle = \sqrt{2}(C_1 - C_2)m_y j + \sqrt{2}C_3 m_z k \quad (10)$$

$$\langle \phi_2 | M | \psi_0 \rangle = \sqrt{2}(C_4 - C_5)m_y j - \sqrt{2}C_6 m_z k \quad (11)$$

$$\text{Im} \langle \psi_1 | \mu | \psi_2 \rangle = (\beta/\hbar)(C_1 C_6 + C_2 C_6 + C_3 C_4 + C_3 C_5) l_x i \quad (12)$$

where  $i$ ,  $j$ , and  $k$  are the unit vectors along the  $x$ ,  $y$ , and  $z$  axes, respectively. If one substitutes eq 10-12 into eq 2, the partial  $B$  term of the lowest  $\pi^* \leftarrow \pi$  transition due to the magnetic mixing of the second  $\pi^* \leftarrow \pi$  state,  $B_{1,2}$ , is obtained to be

$$B_{1,2} = -2(\beta/\hbar) \{ (C_1 - C_2)C_6 + (C_4 - C_5)C_3 \} \{ (C_1 + C_2)C_6 + (C_4 + C_5)C_3 \} m_y m_z l_x / (E_2 - E_1) \quad (13)$$

The value of  $m_y m_z l_x$  is not significantly affected by the aza substitution, and calculated to be positive. Therefore, the sign and magnitude of the partial  $B$  term,  $B_{1,2}$ , are determined by the relative magnitude of the coefficients,  $C_1$ - $C_6$ .

In the cases of  $\alpha$ -azanaphthalenes, the energy difference between two LUMOs,  $\phi_6$  and  $\phi_7$ , is larger than the energy separation between two HOMOs,  $\phi_4$  and  $\phi_5$  (Figure 8). Since the configurational energy of  $\psi_{4 \rightarrow 6}$  is smaller than that of  $\psi_{5 \rightarrow 7}$ , the coefficients  $C_1$  and  $C_4$  are larger than  $C_2$  and  $C_5$ , respec-

Table VII. Wave Functions of the  $\pi^* \leftarrow \pi$  States

Compd	State	Wave function
Quinoline	1st $\pi^* \leftarrow \pi$	$0.73\psi_{4 \rightarrow 6} - 0.65\psi_{5 \rightarrow 7}$
	2nd $\pi^* \leftarrow \pi$	$0.95\psi_{5 \rightarrow 6}$
	3rd $\pi^* \leftarrow \pi$	$0.54\psi_{4 \rightarrow 6} + 0.59\psi_{5 \rightarrow 7} + 0.47\psi_{4 \rightarrow 8}$
	4th $\pi^* \leftarrow \pi$	$0.95\psi_{5 \rightarrow 8}$
	5th $\pi^* \leftarrow \pi$	$0.38\psi_{4 \rightarrow 6} + 0.44\psi_{5 \rightarrow 7} - 0.63\psi_{4 \rightarrow 8}$
	6th $\pi^* \leftarrow \pi$	$0.91\psi_{4 \rightarrow 7}$
Isoquinoline	1st $\pi^* \leftarrow \pi$	$0.44\psi_{4 \rightarrow 6} - 0.61\psi_{5 \rightarrow 7} + 0.62\psi_{5 \rightarrow 6}$
	2nd $\pi^* \leftarrow \pi$	$0.36\psi_{4 \rightarrow 6} - 0.53\psi_{5 \rightarrow 7} - 0.75\psi_{5 \rightarrow 6}$
	3rd $\pi^* \leftarrow \pi$	$0.88\psi_{5 \rightarrow 8}$
	4th $\pi^* \leftarrow \pi$	$0.77\psi_{4 \rightarrow 6} + 0.52\psi_{5 \rightarrow 7} + 0.31\psi_{5 \rightarrow 8}$
	5th $\pi^* \leftarrow \pi$	$0.54\psi_{4 \rightarrow 8} + 0.46\psi_{5 \rightarrow 9} - 0.40\psi_{3 \rightarrow 7}$
	6th $\pi^* \leftarrow \pi$	$0.90\psi_{4 \rightarrow 7}$
Quinoxaline	1st $\pi^* \leftarrow \pi$	$0.83\psi_{4 \rightarrow 6} - 0.53\psi_{5 \rightarrow 7}$
	2nd $\pi^* \leftarrow \pi$	$0.97\psi_{5 \rightarrow 6}$
	3rd $\pi^* \leftarrow \pi$	$0.43\psi_{4 \rightarrow 6} + 0.64\psi_{5 \rightarrow 7} + 0.54\psi_{4 \rightarrow 8}$
	4th $\pi^* \leftarrow \pi$	$0.42\psi_{4 \rightarrow 7} - 0.89\psi_{5 \rightarrow 8}$
	5th $\pi^* \leftarrow \pi$	$0.32\psi_{4 \rightarrow 6} + 0.53\psi_{5 \rightarrow 7} - 0.67\psi_{4 \rightarrow 8}$
	6th $\pi^* \leftarrow \pi$	$0.83\psi_{4 \rightarrow 7} + 0.42\psi_{5 \rightarrow 8}$
Phthalazine	1st $\pi^* \leftarrow \pi$	$0.56\psi_{4 \rightarrow 6} - 0.81\psi_{5 \rightarrow 7}$
	2nd $\pi^* \leftarrow \pi$	$0.96\psi_{5 \rightarrow 6}$
	3rd $\pi^* \leftarrow \pi$	$0.61\psi_{4 \rightarrow 6} + 0.44\psi_{5 \rightarrow 7}$
	4th $\pi^* \leftarrow \pi$	$0.98\psi_{5 \rightarrow 8}$
	5th $\pi^* \leftarrow \pi$	$0.54\psi_{4 \rightarrow 6} - 0.49\psi_{3 \rightarrow 7} + 0.47\psi_{4 \rightarrow 8}$
	6th $\pi^* \leftarrow \pi$	$0.95\psi_{4 \rightarrow 7}$
Quinazoline	1st $\pi^* \leftarrow \pi$	$0.45\psi_{4 \rightarrow 6} - 0.47\psi_{5 \rightarrow 7} + 0.71\psi_{5 \rightarrow 6}$
	2nd $\pi^* \leftarrow \pi$	$0.53\psi_{4 \rightarrow 6} - 0.50\psi_{5 \rightarrow 7} - 0.65\psi_{5 \rightarrow 6}$
	3rd $\pi^* \leftarrow \pi$	$0.54\psi_{4 \rightarrow 6} + 0.49\psi_{5 \rightarrow 7} + 0.40\psi_{4 \rightarrow 8}$
	4th $\pi^* \leftarrow \pi$	$0.33\psi_{4 \rightarrow 6} + 0.44\psi_{5 \rightarrow 7} - 0.78\psi_{5 \rightarrow 8}$
	5th $\pi^* \leftarrow \pi$	$0.54\psi_{4 \rightarrow 8} - 0.44\psi_{5 \rightarrow 8} - 0.44\psi_{5 \rightarrow 9}$
	6th $\pi^* \leftarrow \pi$	$0.85\psi_{4 \rightarrow 7} + 0.36\psi_{3 \rightarrow 6}$
Cinnoline	1st $\pi^* \leftarrow \pi$	$0.47\psi_{4 \rightarrow 6} - 0.49\psi_{5 \rightarrow 7} + 0.69\psi_{5 \rightarrow 6}$
	2nd $\pi^* \leftarrow \pi$	$0.51\psi_{4 \rightarrow 6} - 0.48\psi_{5 \rightarrow 7} - 0.67\psi_{5 \rightarrow 6}$
	3rd $\pi^* \leftarrow \pi$	$0.58\psi_{4 \rightarrow 6} + 0.62\psi_{5 \rightarrow 7}$
	4th $\pi^* \leftarrow \pi$	$0.87\psi_{5 \rightarrow 8}$
	5th $\pi^* \leftarrow \pi$	$0.43\psi_{3 \rightarrow 6} - 0.41\psi_{5 \rightarrow 9} + 0.48\psi_{4 \rightarrow 8}$
	6th $\pi^* \leftarrow \pi$	$0.75\psi_{4 \rightarrow 7} + 0.55\psi_{3 \rightarrow 6}$
Pyrido[2,3- <i>b</i> ]-pyrazine	1st $\pi^* \leftarrow \pi$	$0.82\psi_{4 \rightarrow 6} - 0.38\psi_{5 \rightarrow 7} + 0.36\psi_{5 \rightarrow 6}$
	2nd $\pi^* \leftarrow \pi$	$0.41\psi_{4 \rightarrow 6} - 0.85\psi_{5 \rightarrow 6}$
	3rd $\pi^* \leftarrow \pi$	$0.74\psi_{4 \rightarrow 8} + 0.34\psi_{5 \rightarrow 7} + 0.41\psi_{5 \rightarrow 8}$
	4th $\pi^* \leftarrow \pi$	$0.44\psi_{4 \rightarrow 8} + 0.64\psi_{4 \rightarrow 7} - 0.55\psi_{5 \rightarrow 8}$
	5th $\pi^* \leftarrow \pi$	$0.73\psi_{5 \rightarrow 7} - 0.47\psi_{5 \rightarrow 8}$
	6th $\pi^* \leftarrow \pi$	$0.42\psi_{5 \rightarrow 7} + 0.47\psi_{5 \rightarrow 8} + 0.62\psi_{4 \rightarrow 7}$

tively. Therefore, the resultant sign of  $B_{1,2}$  is negative for  $\alpha$ -azanaphthalenes.

On the contrary, as  $\beta$ -aza substitution lowers the MOs  $\phi_4$  and  $\phi_7$  more effectively than the MOs  $\phi_5$  and  $\phi_6$  (see Figure

8), the configuration  $\psi_{4 \rightarrow 6}$  lies above  $\psi_{5 \rightarrow 7}$ , leading to  $C_2 > C_1$  and  $C_5 > C_4$ . Therefore, the sign of  $B_{1,2}$  of  $\beta$ -azanaphthalene is positive.

**Separate Contributions to the Faraday  $B$  Terms of the Lowest Allowed  $\pi^* \leftarrow \pi$  Transition.** The contributions to the Faraday  $B$  term of the lowest allowed  $\pi^* \leftarrow \pi$  transition from the electronic states are presented in Table VI. The magnetic mixing among  $\pi^* \leftarrow \sigma$  states and the coupling of the  $\pi^* \leftarrow \pi$  state with the ground state do not contribute to the  $B$  terms of the  $\pi^* \leftarrow \sigma$  transitions because the transition electric and magnetic moments in eq 2 and 3 are parallel to each other. The magnetic coupling of the low-lying  $\pi^* \leftarrow \pi$  states with the lowest  $\pi^* \leftarrow \pi$  state is found to be of importance in the  $B$  terms of the lowest  $\pi^* \leftarrow \pi$  transition of azanaphthalenes. There are also significant contributions from the magnetic mixing of the  $\pi^* \leftarrow \pi$  states with the ground state, second, and third terms of eq 1.

## Conclusions

The MCD spectra of some azanaphthalenes were measured in the wavenumber region of 20 000–50 000  $\text{cm}^{-1}$ . Although the sign of the MCD of the lowest allowed  $\pi^* \leftarrow \pi$  transition is positive for all diazanaphthalenes, the MCD signs of two lowest  $\pi^* \leftarrow \pi$  transitions are related to the position of the aza nitrogen atoms.

The Faraday  $B$  terms calculated using the CNDO/S-CI method are in good agreement with the experimental values both in sign and in magnitude. The Faraday  $B$  terms of two lowest  $\pi^* \leftarrow \pi$  transitions are shown to be dominantly induced by the mutual magnetic mixing of two lowest  $\pi^* \leftarrow \pi$  states. The Faraday  $B$  term of the lowest  $\pi^* \leftarrow \pi$  transition originates from the magnetic coupling of low-lying  $\pi^* \leftarrow \pi$  state with the lowest  $\pi^* \leftarrow \pi$  state and the mixing of the  $\pi^* \leftarrow \pi$  states with the ground state.

**Acknowledgment.** The partial support of this work by the Japan Society for Promotion of Science is acknowledged.

## Appendix

**Wave Functions of the  $\pi^* \leftarrow \pi$  States.** The wave functions of the  $\pi^* \leftarrow \pi$  states are given in Table VII, in which  $\psi_{i \rightarrow j}$  represents a electronic configuration arising from one-electron excitation from the MO  $\phi_i$  to the MO  $\phi_j$ .

## References and Notes

- (1) B. Tinland, *Theor. Chim. Acta*, **8**, 361 (1967).
- (2) H. Baba and I. Yamazaki, *J. Mol. Spectrosc.*, **44**, 118 (1972).
- (3) J. E. Ridley and M. C. Zerner, *J. Mol. Spectrosc.*, **50**, 457 (1974).
- (4) (a) D. M. W. van den Ham and D. van der Meer, *Chem. Phys. Lett.*, **12**, 447 (1972); (b) F. Brogli, E. Hellbronner, and T. Kobayashi, *Helv. Chim. Acta*, **55**, 274 (1972).
- (5) A. Tajiri and M. Hatano, *Chem. Phys. Lett.*, **34**, 29 (1975).
- (6) J. Michl, *Chem. Phys. Lett.*, **39**, 386 (1976).
- (7) (a) R. Pariser and R. G. Parr, *J. Chem. Phys.*, **21**, 466, 767 (1953); (b) J. A. Pople, *Trans. Faraday Soc.*, **49**, 1375 (1953).
- (8) (a) J. A. Pople, D. P. Santry, and G. A. Segal, *J. Chem. Phys.*, **43**, S129 (1965); (b) J. A. Pople and G. A. Segal, *ibid.*, **43**, S136 (1965); (c) *ibid.*, **44**, 3289 (1966).
- (9) J. Del Bene and H. H. Jaffé, *J. Chem. Phys.*, **48**, 1807 (1968).
- (10) J. P. Larkindale and D. J. Simkin, *J. Chem. Phys.*, **55**, 5668 (1971).
- (11) R. E. Linder, H. Weller-Feilchenfeld, G. Barth, E. Bunnenberg, and C. Djerrassi, *Theor. Chim. Acta*, **36**, 135 (1974).
- (12) R. E. Linder, E. Bunnenberg, L. Seamans, and A. Moscovitz, *J. Chem. Phys.*, **60**, 1943 (1974).
- (13) (a) J. S. Rosenfield, A. Moscovitz, and R. E. Linder, *J. Chem. Phys.*, **61**, 2427 (1974); (b) J. S. Rosenfield, *J. Chem. Phys.*, **66**, 921 (1977).
- (14) J. S. Rosenfield, *Chem. Phys. Lett.*, **39**, 391 (1976).
- (15) F. M. Sprinkel, D. D. Shillady, and R. W. Strickland, *J. Am. Chem. Soc.*, **97**, 6653 (1975).
- (16) A. Kaito, M. Hatano, and A. Tajiri, *J. Am. Chem. Soc.*, **99**, 5241 (1977).
- (17) J. H. Obbink and A. M. F. Hezemans, *Theor. Chim. Acta*, **43**, 75 (1976).
- (18) A. Kaito and M. Hatano, *J. Am. Chem. Soc.*, submitted for publication.
- (19) (a) P. N. Schatz and A. J. McCaffery, *Q. Rev., Chem. Soc.*, **23**, 552 (1969); (b) P. J. Stephens, *Annu. Rev. Phys. Chem.*, **25**, 201 (1974).
- (20) (a) K. Kimura and M. Kubo, *J. Chem. Phys.*, **32**, 1776 (1960); (b) B. Bak, L. Hansen-Nygaard, and J. Rastrup-Andersen, *J. Mol. Spectrosc.*, **2**, 361 (1958); (c) P. J. Wheatley, *Acta Crystallogr.*, **10**, 182 (1957); (d) *ibid.*, **13**, 80 (1960).
- (21) A. D. Buckingham and P. J. Stephens, *Annu. Rev. Phys. Chem.*, **17**, 399

- (1966).  
 (22) P. O. Löwdin, *J. Chem. Phys.*, **18**, 365 (1950).  
 (23) J. C. Slater, *Phys. Rev.*, **36**, 57 (1930).  
 (24) A. Imamura, T. Hirano, C. Nagata, and T. Tsuruta, *Bull. Chem. Soc. Jpn.*, **45**, 396 (1972).  
 (25) M. Suzuki, Y. Nihel, and H. Kamada, *Bull. Chem. Soc. Jpn.*, **42**, 323 (1969).  
 (26) L. Seamans and A. Moscovitz, *J. Chem. Phys.*, **56**, 1099 (1972).  
 (27) D. J. Caldwell and H. Eyring, *J. Chem. Phys.*, **58**, 1149 (1973).  
 (28) (a) R. W. Glass, L. C. Robertson, and J. A. Merritt, *J. Chem. Phys.*, **53**, 3857 (1970); (b) G. Fischer, A. D. Jordan, and I. G. Ross, *J. Mol. Spectrosc.*, **40**, 397 (1971).  
 (29) Y. Hasegawa, Y. Amako, and H. Azumi, *Bull. Chem. Soc. Jpn.*, **41**, 2608 (1968).  
 (30) S. C. Wait, Jr., and F. M. Grogan, *J. Mol. Spectrosc.*, **24**, 383 (1967).  
 (31) R. M. Hochstrasser and C. Marzacco, *J. Chem. Phys.*, **48**, 4079 (1968).  
 (32) R. M. Hochstrasser and D. A. Wiersma, *J. Chem. Phys.*, **56**, 528 (1972).  
 (33) The  $y$  and  $z$  axes are chosen as the long and short axes, respectively, of naphthalene, and the  $x$  axis is set perpendicular to the molecular plane.  
 (34) J. R. Platt, *J. Chem. Phys.*, **17**, 484 (1949).  
 (35) J. Michl, *J. Chem. Phys.*, **61**, 4270 (1974).

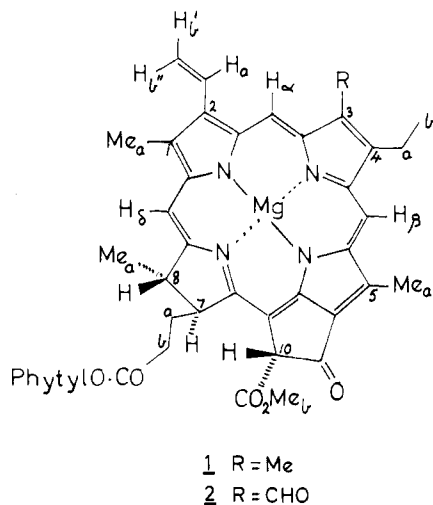
## Hyperfine Coupling in Chlorophyll Radical Cations. A Nuclear Magnetic Resonance Approach

John C. Waterton and Jeremy K. M. Sanders\*

Contribution from the University Chemical Laboratory,  
Cambridge CB2 1EW, United Kingdom. Received October 19, 1977

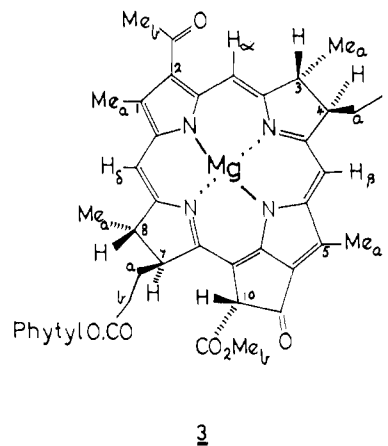
**Abstract:** Most of the relative proton hyperfine coupling constants in the radical cations of chlorophyll a, chlorophyll b, and bacteriochlorophyll a have been determined using electron transfer NMR line broadening in the fast exchange limit. The results have been used to confirm ENDOR assignments for some methyl groups and to give a detailed spin density distribution for many positions exhibiting no ENDOR signals. Agreement with ENDOR is qualitatively good for Chl a and Bchl a, but is poor for Chl b.

In photosynthesis, light energy from the sun is trapped as chemical energy in the form of reducing power. In the first few nanoseconds after light absorption an electron is ejected from a reaction-center chlorophyll-protein complex and a chlorophyll radical cation is produced.<sup>1,2</sup> The reaction center chlorophyll of plant photosynthesis is chlorophyll a (1), which may be accompanied by the accessory chlorophyll b (2); pho-



tosynthetic bacteria employ bacteriochlorophyll a (3) or bacteriochlorophyll b ( $\Delta^{4,4a}3$ ).

Although chlorophyll radical cations play a central role in photosynthesis, elucidation of their properties is made difficult by their chemical instability and the limitations of the techniques normally used to study them. Thus, their ESR spectra generally consist of a single Gaussian signal containing over  $10^9$  unresolved lines<sup>3</sup>, and at the outset of this work ENDOR was giving only rudimentary information.<sup>4</sup> Progress has been rapid in both techniques recently<sup>5-7</sup> but each suffers a fundamental limitation: assignment of hyperfine coupling constants to individual protons requires deuteration, chemical modifi-



cation, or fitting observed couplings to those predicted by MO theory.

In contrast, the NMR spectra of chlorophylls are rich in information, can be assigned *spectroscopically* without recourse to modification,<sup>8</sup> and can yield relative hyperfine coupling constants via electron transfer broadening. This technique has been known for many years,<sup>9</sup> the theory is well established,<sup>10</sup> and its use in assigning ESR spectra has been advocated,<sup>11</sup> but it has been largely ignored. We show here<sup>12</sup> that the method can be used successfully in systems which are much more complex than those<sup>13</sup> previously studied. It should be applicable also to the recently synthesized "reaction-center" dimers,<sup>14-17</sup> and the equally significant radical anions.<sup>18</sup> A similar technique is being used to study chlorophyll triplets.<sup>19</sup>

### Theory

Spin densities ( $\rho_c$ ) on carbon atoms in a  $\pi$  radical can in principle be determined from proton hyperfine coupling constants ( $a_H$ ) via the McConnell relation (eq 1) where  $Q$  is a parameter which reflects the efficiency of spin transmission